Internship Report

ASELSAN BILKENT MIKRO NANO TEKNOLOJILERI SAN. VE TIC. A.Ş.

MANUFACTURING PROCESS AND CHARACTERIZATION OF A COMMERCIAL PHOTODIODE

July, 2025

Nazlıcan Yıldırım
Middle East Technical University
Faculty of Arts and Science
nazlican.yildirim@metu.edu.tr

Contents

1 Introduction **1**

2 Packaging a Photo Diode **1**
2.1 Wafer Dicing 2
2.2 Die Bonding 3
2.3 Wire Bonding 4

3 Methodology for Characterization **5**
3.1 Dark current 5
3.1.1 What is dark current? 5
3.1.2 How can dark current be measured? 5
3.2 Responsivity 6
3.2.1 What is responsivity? 6
3.2.2 How can responsivity be measured? 7
3.3 Capacitance 8
3.3.1 What is capacitance? 8
3.3.2 How can junction capacitance be measured? 8
3.4 Response Time 9
3.4.1 What is response time? 9
3.4.2 How can response time be measured? 10
3.5 Transmission Line Method (TLM) 10
3.5.1 What is TLM? 11
3.5.2 How can TLM be measured? 12

4 Experimental Results **13**

5 Discussion **16**

References **19**

1 Introduction

Photodetectors are devices that convert photonic energy into electrical energy [1]. This conversion relies on the photoelectric effect, which can occur through two mechanisms: the *external photoelectric effect* (emission of electrons from a surface) and the *internal photoelectric effect* (generation of charge carriers within a material). Photodiodes operate on the basis of the internal photoelectric effect and utilize an electron-hole pair generation mechanism [2]. They are widely used in optical communication, sensing, and imaging systems due to their high sensitivity and fast response.

In both research and industrial applications, proper packaging and electrical characterization are essential to ensure reliable device performance. This report aims to present a complete workflow for both the fabrication and validation of a commercial photodiode.

To evaluate the characteristic properties of the photodiode, several tests must be conducted during both fabrication and R&D stages. This report focuses on two main aspects:

- The packaging of a commercial photodiode (including wafer dicing, die bonding, and wire bonding)
- The electrical and optical characterization of the photodiode (including dark current, responsivity, capacitance, response time, etc.)

During the internship, the complete manufacturing steps of a commercial silicon photodiode were observed. Except for TLM characterization, all measurements in this study were performed using a **Hamamatsu S2744-09**, a planar-type silicon PIN photodiode optimized for near-infrared applications. The experimental results were compared with the specifications provided in the manufacturer's datasheet [3].

2 Packaging a Photo Diode

The wafer can be obtained through the wafer slicing process. During my internship, the wafers were purchased from different manufacturers. To fabricate a photodiode from a silicon wafer, two different approaches can be followed. One of these approaches is the packaging of a commercial photodiode, which consists of four main stages: wafer dicing, die bonding, wire bonding, and welding. This report focuses on the first three stages. The other approach is the characterization of a photodiode.

2.1 Wafer Dicing

Wafer dicing is the process of separating silicon wafers into individual dies. To achieve this, three common methods can be used: blade dicing, laser dicing, and plasma dicing. The decision on which type of dicing method to use depends on the properties of the wafer and the desired outcomes. For instance, when considering laser dicing, it is important to ensure that the semiconductor material is not affected by the laser's wavelength. During my internship, blade dicing was used, and the procedure for this method was as follows:

- **Blade Dicing:** Blade dicing is a mechanical technique in which a high-speed rotating diamond blade cuts the wafer and separates it into individual dies. The achievable die size can vary depending on the blade material and its radius. For example, in the Disco DAD 3220 system, dies as large as 6 x 6 inches can be produced [4]. However, there are some limitations. These include increased mechanical stress on the material, and challenges in producing densely packed small dies. Additionally, during the cutting process, the temperature may increase, potentially causing thermal damage to the wafer. The process consists of three main stages, which are described in the procedure section below.

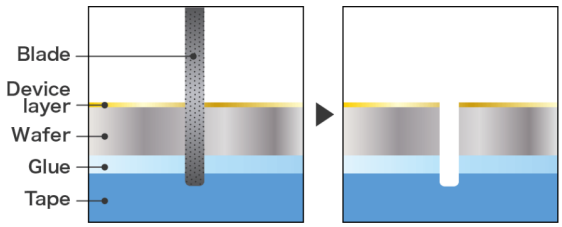

Figure 1: Scheme of a blade dicing machine and the layers [5]

Procedure

1. Before dicing, the wafer should be glued onto a tape to prevent it from breaking. The type of tape used depends on the wafer material. For example, for silicon wafers, UV-sensitive plastic tape is commonly used.

2. Cutting alignments and die shapes are manually arranged on the machine before starting the process. After alignment in terms of angle and channels, the wafer is diced in a deionized water environment to minimize temperature rise and reduce debris.

3. After cutting is completed, the wafer-tape assembly is exposed to UV light. UV exposure weakens the adhesive, allowing the tape and the wafer to be easily separated.

2.2 Die Bonding

Die bonding is a critical step in semiconductor packaging where individual semiconductor dies, separated from a processed wafer during the dicing step, are attached to a substrate or package base such as a header, ceramic carrier, or PCB. The primary goals of die bonding are to provide mechanical support, ensure thermal conductivity for heat dissipation, and enable reliable electrical connections through subsequent interconnection processes such as wire bonding.

There are several die bonding techniques depending on the application requirements, device materials, and production volume. The three most common methods are eutectic bonding, epoxy bonding, and solder bonding.During the internship, the epoxy die bonding technique was learned and applied to attach the photodiode die to its package.

- **Epoxy bonding**, particularly with epoxy-based die attach materials, is the most prevalent method in high-volume manufacturing. Thermosetting epoxies or conductive pastes are dispensed or stencil-printed onto the substrate, and the die is placed and cured under controlled temperature and pressure. This approach offers low processing temperatures, cost efficiency, and good mechanical adhesion.

Die bonding also involves precise alignment of the die to the pad or frame on the substrate. This alignment must meet micron-level tolerances, especially for multi-die systems. The bonding process may be performed in ambient conditions, vacuum, or inert gas environments (e.g., nitrogen) depending on the sensitivity of the materials used.

In conclusion, die bonding is a multifaceted essential process that directly influences the mechanical reliability, electrical performance, and thermal management of the packaged device. The choice of bonding technique and materials must be carefully optimized based on device application, manufacturing scalability, and cost constraints.

The die bonding process is a critical step in semiconductor packaging, where the photodetector die is attached to the substrate using a conductive adhesive. The procedure is typically carried out using a die bonder machine and involves the following section.

Procedure

1. A silver-filled epoxy adhesive is applied to predefined areas on the substrate (mask holder), typically via stencil printing or dispensing techniques.

2. Photodetector dies are loaded onto designated die holders inside the die bonder machine. The system is operated under vacuum conditions to prevent contamination and ensure precise handling.

3. The machine scans the positions of both the substrate and the dies using an integrated vision system. Then, utilizing a vacuum-based pick-up tool, it sequentially picks up each die and accurately places it onto the epoxy-applied area on the substrate. The placement is performed with micrometer-level precision to avoid mechanical damage and ensure optimal alignment.

2.3 Wire Bonding

Wire bonding is the most widely used method for establishing electrical interconnections between the silicon die and the package or lead frame in semiconductor devices. It is a key step in microelectronic packaging due to its relatively low cost, process flexibility, and compatibility with a wide range of materials and geometries [6]. Gold, aluminum, and copper wires are commonly used, depending on the application and compatibility with bonding surfaces. There are two types of wire bonding, ball bonding and wedge bonding.

- **Ball Bonding:** Predominantly used with gold wires. A small ball is formed at the wire tip using an electric flame-off (EFO) process [7]. The ball is bonded to the die pad using ultrasonic energy and pressure. Then, the wire is looped to the second bonding site, where a stitch bond is formed on the package lead.

- **Wedge Bonding:** Typically uses aluminum or copper wires. A wedge-shaped tool presses the wire onto the bonding surface at both ends, forming two wedge bonds without a ball. Wedge bonding generally requires more precise alignment and motion control due to its dependence on bonding angle and wire orientation.

According to industry estimates, over 95% of all wire bonds in IC packaging utilize gold ball bonding due to its high-speed capability and ease of automation [6]. Ball bonding requires three-axis control (X, Y, Z), while wedge bonding requires an

additional rotational (θ) axis, making it more complex and slower in high-volume manufacturing settings.

Wire bonding faces several challenges, especially as semiconductor devices scale down in size and increase in complexity. As die pads become smaller and more densely packed, precise control of pressure and ultrasonic energy becomes crucial to avoid damaging fragile circuits.

In this project, gold ball bonding to connect the pad of photodiode to the package lead was performed. The wire bonding machine formed a 25 μm diameter gold wire ball bond on the die pad, then a wedge bond on the lead frame.

3 Methodology for Characterization

Characterization of a photodiode determines its properties using electrical, optical, and I-V characterization methods. This report focuses only on the dark current, capacitance, and response time for electrical characterization and responsivity for optical characterization of a commercial photodiode.

3.1 Dark current

3.1.1 What is dark current?

Dark current refers to the electrical current that flows through a photosensor in the absence of light [8]. It is measured in amperes (A). In an ideal photodiode, this current should be zero, but due to thermal excitation and junction leakage in the semiconductor, a non-zero current is always present. Due to thermal excitation, the dark current increases exponentially.

3.1.2 How can dark current be measured?

During the experiment, a Keithley source meter, connecting cables, a photodiode, and a printed circuit board (PCB) were utilized. A schematic representation of the setup is shown in Figure 2. In this configuration, Channel A of the source meter was connected to supply the bias voltage to the PCB, while Channel B was responsible for measuring the current. The bias voltage was applied to the PCB, allowing the applied voltage to effectively cover the entire plate.

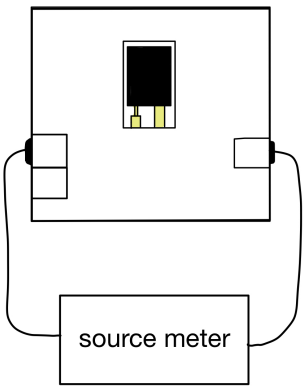

Figure 2: Dark Current Setup Schema

To measure the dark current of the photodiode, the experimental setup shown in Figure 2 was used. Before measurement, a reverse bias voltage of 70 V was applied. The photodiode was first inserted into the designated pin sockets on the PCB. Initially, the photocurrent was measured under ambient light to establish a baseline. Then, a light-blocking cap was placed over the photodiode to eliminate all incident light. After the current was allowed to stabilize, the resulting steady-state current was recorded as the dark current of the device.

3.2 Responsivity

3.2.1 What is responsivity?

Responsivity defines the output current generated per unit of incident optical power, and is expressed in Amperes per Watt (A/W), which is represented in Equation 4 [9]. It depends on the material properties of the sensor and varies with the wavelength of the incident light [10].

For a known photosensor, the responsivity can be obtained directly from the manufacturer's datasheet. For an unknown sensor, it can be calculated experimentally using Equation 2. By measuring the dark current (the current in the absence of light) and the photocurrent (the current when the light source is on), the optical power incident on the photodetector can be used to determine its responsivity.

$$R = \frac{I}{P} \tag{1}$$

$$R(\lambda) = \frac{(I_{\text{photon}} - I_{\text{dark}})(\lambda)}{P_{\text{optical}}(\lambda)} \tag{2}$$

3.2.2 How can responsivity be measured?

To measure the responsivity of a photodiode, an optical power meter, a PCB, a photosensor, connection cables, and a laser source were used. The experimental setup is shown in Figure 3.

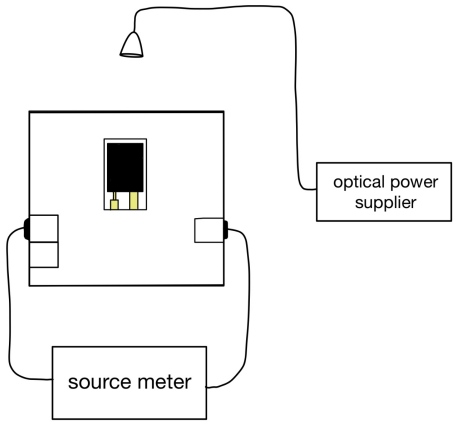

Figure 3: Responsivity Setup Schema

The first channel is connected to the bias input of the PCB, and a bias voltage of 70 V is applied. The second channel is used to measure the current output. A laser source with a wavelength of 1064 nm was used as the optical input in this experiment. The laser beam was manually aligned onto the photodiode for maximum illumination. The incident optical power was measured using the power meter, and the corresponding photocurrent was recorded for responsivity calculation.

For calculating responsivity using Equation 3, the dark current of the photodiode (with the laser off) that was measured was taken into account. Then, the laser was turned on and the photocurrent measured. The responsivity was calculated from the difference, using Equation 3.

3.3 Capacitance

3.3.1 What is capacitance?

The capacitance of a photodiode is created by its depletion region, which is inversely related to reverse bias voltage. When reverse-bias voltage is increased, the capacitance of the depletion region is decreased, and visa versa. There are two types of capacitance of a junction capacitance.

- Diffusion Capacitance(Cd)
- Transition Capacitance(Ct)

In the p-n junction, there can be two different kinds of capacitance: diffusion capacitance and transition (junction) capacitance because of the biasing conditions.

Under forward bias, the dominant capacitance is diffusion capacitance (C_D), which results from the storage of minority carriers near the depletion region. This stored charge leads to a significant capacitive effect, which is typically much larger than the transition capacitance [11]. Therefore, predominantly considered in forward-biased operation.

Conversely, in reverse bias, the dominant mechanism is transition capacitance (C_T), also referred to as depletion capacitance or barrier capacitance. In this case, the p-type and n-type regions act as the conductive plates of a parallel-plate capacitor. As the voltage of reverse bias increases, the width of the depletion widens and the effective area of the conductive regions narrows, leading to a decrease in the transition capacitance [12]. This inverse relationship between reverse bias voltage and capacitance is a key characteristic of junction diodes.

While a small amount of transition capacitance exists even under forward bias, it is typically negligible compared to the much larger diffusion capacitance.

3.3.2 How can junction capacitance be measured?

Junction capacitance were measured under varying reverse bias voltages that was 5 V to 40 V with 5 V steps to observe how the capacitance changes with bias. The setup schema can be seen in Figure 4. To perform the experiment, wires, LCR meters, and a photodiode were used. In Figure 4, the photodiode leads are drawn with different lengths to indicate polarity. The longest lead was connected to the LCR meter's biased terminal, and the shorter lead to the ground terminal.

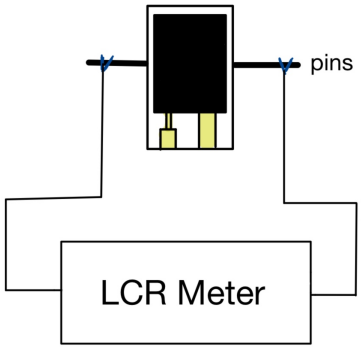

Figure 4: The setup schema for measuring junction capacitance

The voltage-dependent capacitance characteristics of photodiodes can be described by Equation 3, where the built-in potential is denoted by V_{Bi}, and all other parameters represent known physical constants under standard conditions [13].

$$\frac{1}{C^2} = \left(\frac{2}{\varepsilon_0 \varepsilon_s q N d A^2}\right)\left(V_{Bi} - V - \frac{kT}{q}\right) \tag{3}$$

In this expression, ε_0 represents the vacuum permittivity, while ε_s denotes the relative permittivity of the semiconductor material. The symbol q refers to the elementary charge, and N is the doping concentration of the semiconductor. The parameter d corresponds to the depletion width, and A is the junction area. V denotes the externally applied bias voltage, k is Boltzmann's constant, and T represents the absolute temperature.

Equation 3 implies that a plot of $1/C^2$ versus applied voltage V yields a linear relationship which can be exploited to determine important device parameters such as the built-in potential and the doping profile.

3.4 Response Time

3.4.1 What is response time?

Response time is the time interval between the application of an optical signal to a photodetector and the corresponding change in its electrical output. It defines how quickly the photodetector can respond to a varying optical input and is a critical parameter in high-speed applications.

The response time is characterized by two related metrics: rise time and fall time. The rise time refers to the time it takes for the output signal to increase from 10

to 90 of its maximum value after a sudden increase in illumination. Conversely, the fall time measures the time it takes for the signal to decrease from 90 to 10 of its maximum value after the illumination is removed [14].

Several factors influence the response time, carrier transit time, RC time constant, diffusion time, junction capacitance and resistance of the detector structure. Minimizing the response time is crucial to maximize speed performance, and this is often achieved through design optimizations such as reducing junction capacitance or increasing bias voltage to widen the depletion region.

3.4.2 How can response time be measured?

The response time of the photodiode, including both the rise time and fall time, was measured using the experimental setup illustrated in Figure 5. The system consisted of an optical power source, a source meter, a printed circuit board (PCB), the photodiode under test, an oscilloscope, and appropriate connecting cables. A quasi-continuous wave (QCW) pulsed light source was used. The pulse profile and power were first verified using a fast InGaAs photodiode (calibration detector) before measuring the response of our photodiode. During the measurements, a bias voltage of 70 V was applied to the photodiode.

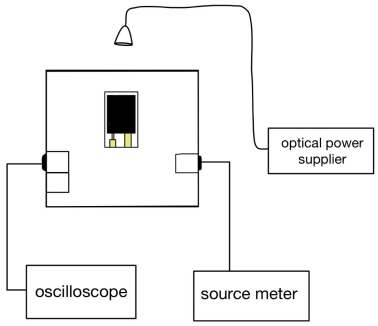

Figure 5: Response Time Setup Schema

3.5 Transmission Line Method (TLM)

The Transmission Line Method (TLM), also known as the transfer length method, is not always included in standard photodiode characterization procedures; however, it is a valuable and necessary technique for evaluating contact and sheet resistance.

During the internship, a wafer die was used to practice using the probe station and to perform TLM measurements.

3.5.1 What is TLM?

The Transmission Line Method (TLM) is a widely adopted technique for the electrical characterization of alloyed ohmic contacts. It facilitates the experimental determination of two critical parameters: the specific contact resistance (ρc) and the sheet resistance (R_C) of the underlying semiconductor layer beneath the contact interface [15]. To implement this method, a probe station and a wafer were used. Rectangular metal pads patterned on the surface of the wafer were employed to measure the contact resistance value.

Top View of the Wafer Region Used for TLM

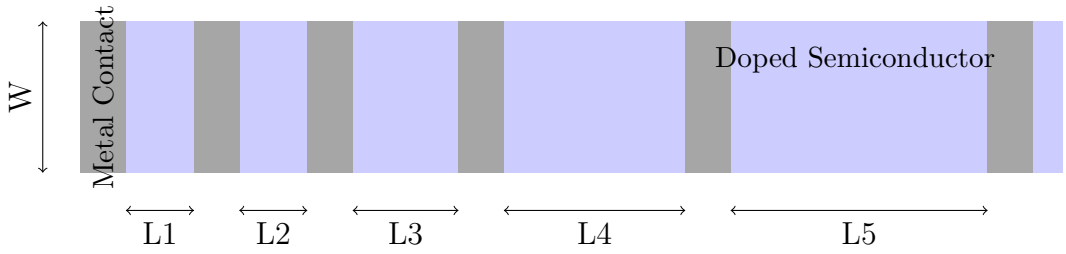

The total resistance between two pads can be expressed as Equation 6, where R_C is the contact resistance, R_S is the sheet resistance, W is the width of the contact pad, L is the distance between adjacent pads.

The slope of the R_{total} versus L graph corresponds to R_S/W, and the y-intercept gives $2R_C$. Once the slope is determined from the linear fit, the sheet resistance R_S can be calculated using:

$$R_S = \text{Slope} \times W \tag{4}$$

$$R_{\text{total}} = 2R_C + \left(\frac{R_S}{W}\right) \cdot L \tag{5}$$

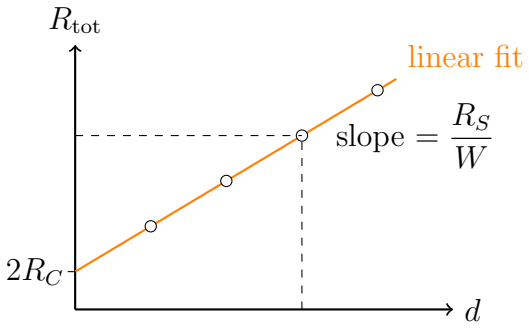

Figure 6: Linear fit in the Transfer Length Method (TLM)

3.5.2 How can TLM be measured?

To characterize the resistance of a photodiode, the Transmission Line Method (TLM) can be utilized in conjunction with a probe station, as shown in Figure 7. A probe station is a precision instrument designed to measure electrical parameters such as voltage and current through microscopic probes. These probes must make physical contact with the metal pads of the photodiode with proper alignment and controlled pressure.

Improper alignment or excessive pressure applied by the probes can lead to surface damage, such as scratches or cracks on the sensitive layers of the photodiode. Alignment can be done manually via micromanipulators or by automated control, depending on the system.

Once the probes are properly positioned, the electrical measurements are carried out and transmitted to a connected computer system for data acquisition. This data is essential for further analysis, including the extraction of contact resistance and sheet resistance using the TLM approach.

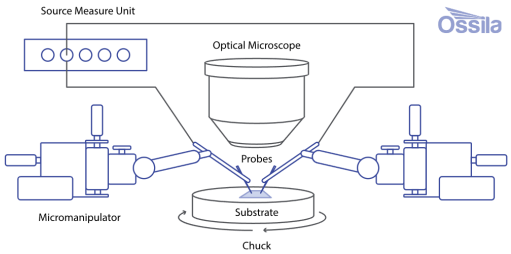

Figure 7: Description of a Probe Station [16]

Procedure

1. The photodiode is placed carefully onto the chuck of the probe station using nonmetallic forceps. Once positioned, the vacuum system is activated to stabilize the sample on the chuck.

2. The optical microscope and probe tips are aligned precisely to ensure contact with the appropriate metal contact pads of the photodiode. Care must be taken to avoid damaging the surface during alignment.

3. The measurement software is launched, and appropriate voltage or current sweep parameters are configured. The electrical signals are then applied to the photodiode, and the corresponding resistance and voltage values are recorded in real time by the connected system.

4 Experimental Results

Dark Current and Responsivity

In the dark current measurement, dark current of the photodiode was found to be 4.0 nA at a reverse bias of 70 V (using the procedure described in Section 3.1.2). For the responsivity measurement, the laser's optical power was 4.2 mW at 1064 nm, and photocurrent of the the photodiode was 800 µA under 70 V bias. Using these values in Equation (3), the responsivity was calculated to be 0.190 A/W. The calculation is as follows:

$$R = \frac{800 * 10^{-6}}{4.2 * 10^{-3}}$$

$$R = 0.190 A/W$$

Capacitance

The measurement of the capacitance with respect to reverse bias voltage was recorded, and it can be seen in Table 1.

	Reverse Bias Voltage (V)	Capacitance (pF)
1	5	222.0
2	10	163.5
3	15	136.3
4	20	119.6
5	25	108.2
6	30	99.6
7	35	92.9
8	40	87.6

Table 1: Capacitance vs. Reverse Bias Voltage Measurements

Using these data, a graph of capacitance vs. reverse voltage was plotted (Figure 8). The curve follows approximately a $1/\sqrt{V}$ dependence, as expected for a parallel-plate depletion capacitance.

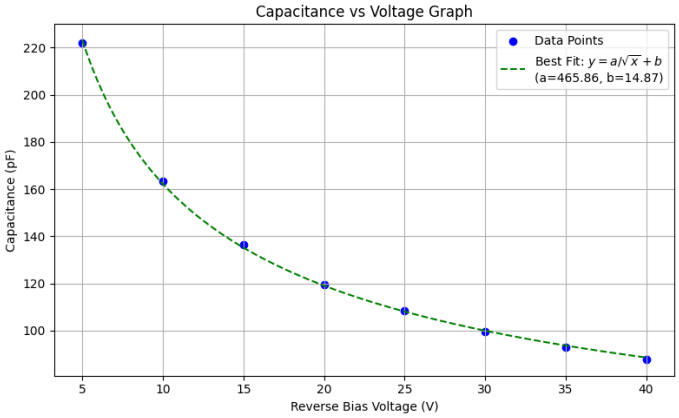

Figure 8: Capacitance vs Reverse Bias Graph

According to Equation (4), a plot of $1/C^2$ vs V should yield a straight line from which the built-in potential can be extracted. The data roughly aligns with this theory.

Response Time

During the measurements, the properties of the QCW was aligned as in below.

- Pulse Period = 20 ms
- Pulse Width = 5 ms

- Frequency = 50 Hz
- Duty Cycle = 25%

Measured rise time of the photodiode was 36.4 µs and fall time 18.7 µs. The waveform of the photodiode can be seen in Figure 9.

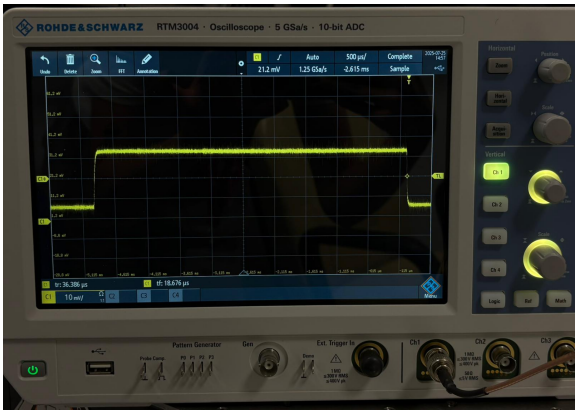

Figure 9: Response waveform of the photodiode

Transmission Line Method

The data of the wafer that is obtained from probe station is in Table 1. Using Python, the slope of the resistance vs length graph was computed, and found as 0.01967 Ω/µm that can be seen in Figure 10. The code for the figure is in Appendix.

	Length (µm)	Resistance (Ω)
1	500	9.608
2	400	8.657
3	300	6.642
4	200	4.519
5	100	2.321
6	50	1.235
7	20	0.597

Table 2: Length and Resistance Measurements of Photodiode

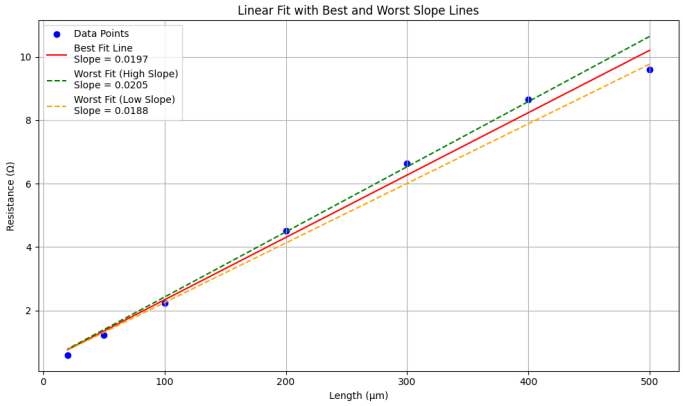

Figure 10: Determining resistance using TLM.

The width of the metals are 300 µm.

Then R_S was calculated as 5.91 Ω per square using Equation 5.

The y-intercept was 0.40Ω, indicating an extremely low contact resistance 0.2Ω for each pad.

5 Discussion

In this section, the characterization results of the packaged silicon photodiode are interpreted and compared with expected performance values. All experiments were conducted at room temperature under a reverse bias of 70 V unless otherwise stated. Potential error sources are identified, and improvements are suggested for measurement techniques.

The dark current of the photodiode was measured as **4.0 nA**, which is exceptionally low and consistent with the expected values given in the datasheet[3]. Such a low dark current indicates high junction quality and minimal leakage, confirming the success of the fabrication and packaging process.

The responsivity was calculated as **0.190 A/W** at a wavelength of 1064 nm. According to the manufacturer's datasheet, the expected responsivity is approximately **0.200 A/W**, resulting in a **5% error**. This discrepancy can be attributed to several factors such as manual alignment of the laser beam, uncertainties in the optical power calibration, or slight variations in the photodiode's surface area exposed to light. Despite this minor error, the measured responsivity is within acceptable limits and confirms that the photodiode is suitable for optical sensing applications in the near-infrared range.

The **capacitance-voltage (C-V)** measurements revealed a clear decrease in junction capacitance with increasing reverse bias, ranging from 222.0 pF at 5 V to 87.6 pF at 40 V. This behavior is consistent with the theoretical model where the depletion region widens with reverse bias. The experimental data align well with a trend $1/\sqrt{V}$, as shown in Figure 8, which confirms the expected junction behavior. These results also indicate that the device is fully depleted at the operating voltage, which is ideal for maximizing quantum efficiency and reducing response time.

The **response time** of the photodiode was measured as **36.4** μ**s** for rise time and **18.7** μ**s** for fall time. These values indicate that the device is suitable for low-frequency or DC applications, such as power monitoring or slow optical modulation. The relatively slow response is attributed to the large junction area and associated capacitance, as well as carrier diffusion dynamics. Faster photodiodes would require smaller active areas or avalanche gain structures, which were beyond the scope of this project.

The Transmission Line Method (TLM) characterization yielded a **sheet resistance** of approximately **3.93** Ω and a **contact resistance** of **0.2** Ω per pad. These values indicate excellent ohmic contact and low series resistance, confirming that the wire bonding and die-attachment processes did not introduce significant parasitic losses. The linearity of the resistance vs. distance graph also confirms the uniformity of the semiconductor layer and the effectiveness of the metalizing process.

In conclusion, the project successfully demonstrated the full fabrication and characterization of a commercial silicon photodiode. The performance of the device aligns well with the theoretical expectations and datasheet values. Dark current and contact resistance values were exceptionally low, while responsivity and capacitance results confirmed proper device operation. Although the response speed limits its use in high-frequency applications, the photodiode remains effective for a broad range of sensing tasks. Future improvements could include automated optical alignment, full encapsulation for environmental protection, and temperature-dependent characterization to further validate device reliability.

References

[1] Roman A. Surmenev and Maria A. Surmeneva. "The influence of the flexoelectric effect on materials properties with the emphasis on photovoltaic and related applications: A review". In: *Materials Today* 67 (2023), pp. 256–298. ISSN: 1369-7021. DOI: https://doi.org/10.1016/j.mattod.2023.05.026. URL: https://www.sciencedirect.com/science/article/pii/S1369702123001773.

[2] Venkatarao Selamneni and Parikshit Sahatiya. "Mixed dimensional Transition Metal Dichalcogenides (TMDs) vdW Heterostructure based Photodetectors: A review". In: *Microelectronic Engineering* 269 (2023), p. 111926. ISSN: 0167-9317. DOI: https://doi.org/10.1016/j.mee.2022.111926. URL: https://www.sciencedirect.com/science/article/pii/S0167931722002209.

[3] Hamamatsu Photonics K.K. *Silicon PIN Photodiodes S2744-08, S2744-09 Datasheet*. 2023. URL: https://www.hamamatsu.com/content/dam/hamamatsu-photonics/sites/documents/99_SALES_LIBRARY/ssd/s2744-08_etc_kpin1049e.pdf.

[4] DISCO Corporation. *Dicing saw DAD3220*. https://www.disco.co.jp/eg/products/dicer/dad3220.html. n.d.

[5] DISCO. *Basic Process Using Blade Dicing Saws*. https://www.disco.co.jp/eg/solution/library/dicing/basic.html. n.d.

[6] Jianbiao Pan and Patrice Fraud. "Wire bonding challenges in optoelectronics packaging". In: *Proceedings of the 1st SME Annual Manufacturing Technology Summit*. Dearborn, MI, Aug. 2004.

[7] K. Finney. *Ball Bonding and the Electronic Flame-Off Process*. https://www.palomartechnologies.com/blog/ball-bonding-and-the-electronic-flame-off-process. Accessed: 2025-07-26. Oct. 2016.

[8] Dominic Kwan et al. "Recent trends in 8–14 m type-II superlattice infrared detectors". In: *Infrared Physics Technology* 116 (2021), p. 103756. ISSN: 1350-4495. DOI: https://doi.org/10.1016/j.infrared.2021.103756. URL: https://www.sciencedirect.com/science/article/pii/S1350449521001286.

[9] Krishan Kumar and Davinder Kaur. "A review on recent advancements in the growth of MoS2 based flexible photodetectors". In: *Solar Energy Materials and Solar Cells* 268 (2024), p. 112736. ISSN: 0927-0248. DOI: https://doi.org/10.1016/j.solmat.2024.112736. URL: https://www.sciencedirect.com/science/article/pii/S0927024824000485.

[10] Zbigniew Bielecki et al. "Review of photodetectors characterization methods". In: *Bulletin of the Polish Academy of Sciences. Technical Sciences* 70.2 (2022).

[11] Zbigniew Bielecki et al. “Review of photodetectors characterization methods”. In: *Bulletin of the Polish Academy of Sciences, Technical Sciences* 70 (May 2022). DOI: 10.24425/bpasts.2022.140534.

[12] Vasco D.B. Bonifacio and Rita F. Pires. “Photodiodes: Principles and recent advances”. In: *Materials NanoScience* 6.2 (July 2019), pp. 38–46. URL: https://pubs.thesciencein.org/journal/index.php/jmns/article/view/235.

[13] Fatih Kara. “Fe KATKILI TiO2 İNCE FİLMLERİN ÜRETİMİ VE OPTİK ÖZELLİKLERİ”. MA thesis. Kırklareli Üniversitesi, 2020.

[14] Alexander O. Goushcha and Bernd Tabbert. “On response time of semiconductor photodiodes”. In: *Optical Engineering* 56.9 (2017), p. 097101. DOI: 10.1117/1.OE.56.9.097101. URL: https://doi.org/10.1117/1.OE.56.9.097101.

[15] Geoffrey K. Reeves, Patrick W. Leech, and H.Barry Harrison. “Understanding the sheet resistance parameter of alloyed ohmic contacts using a transmission line model”. In: *Solid-State Electronics* 38.4 (1995), pp. 745–751. ISSN: 0038-1101. DOI: https://doi.org/10.1016/0038-1101(94)00234-7. URL: https://www.sciencedirect.com/science/article/pii/0038110194002347.

[16] Oscilla. *What is probe station?* URL: https://www.ossila.com/pages/what-is-a-probe-station.